A Unique Method for Laboratory Quantification of Gaseous Nitrous Acid (HONO) Using the Reaction HONO + HCl → ClNO + H_2O

Lisa M. Wingen, William S. Barney, Matthew J. Lakin, Theo Brauers,† and Barbara J. Finlayson-Pitts*

Department of Chemistry, University of California, Irvine, Irvine, California 92697-2025

Received: August 16, 1999; In Final Form: October 29, 1999

Although the formation and reactions of gaseous nitrous acid (HONO) in the atmosphere are of great interest, it is difficult to accurately measure HONO both in the atmosphere and in laboratory systems. We report a new technique for quantifying gaseous HONO in laboratory systems. The method utilizes the reaction of gas phase HONO with an excess of HCl gas to produce nitrosyl chloride (ClNO), which is readily quantified using FTIR. HONO was formed by flowing N_2 over the surface of an aqueous HCl solution and through a bed of $NaNO_2$, then directly into a 561 L chamber. An excess of gaseous HCl was added to the chamber to initiate the reaction in N_2 at room temperature and 1 atm total pressure. The loss of HONO was followed by DOAS and FTIR and the formation of ClNO was measured by FTIR. While direct measurement of HONO by FTIR is limited by uncertainties in the available infrared absorption cross sections, calibration for ClNO is readily carried out since ClNO can be synthesized with high purity. The stoichiometry for ClNO formed to HONO reacted was determined to be 0.9 ± 0.2 (1σ). The concentration−time profiles for both HONO and ClNO were fitted with a kinetics model which gave a rate constant for the reaction HONO + HCl $\xrightarrow{k_1}$ ClNO + H_2O of $k_1 \leq (1.9 \pm 1.3) \times 10^{-19}$ cm^3 molecule^{-1} s^{-1} (2σ) at 297 K. This should be taken as the upper limit for the gas phase reaction since some contribution from heterogeneous reaction at the chamber walls cannot be conclusively ruled out.

I. Introduction

Nitrous acid (HONO) photodissociation has been found to be the predominant source of OH in the early morning in some urban areas.[1−3] The reaction of HONO on surfaces[4−6] to produce N_2O may also contribute to the atmospheric sources of N_2O, a greenhouse gas which also contributes to stratospheric ozone cycles[7,8] and for which there are still large uncertainties in many of its sources.[7,9,10] In addition, HONO has direct and indirect health effects,[11,12] which is of particular concern indoors where elevated HONO levels have been found.[13−17] HONO is also known to react with secondary and tertiary amines to form carcinogenic nitrosamines.[18]

The nighttime concentration of HONO has been measured to reach up to 10−15 ppb in heavily polluted areas.[2,19−22] Potential sources of HONO that have been proposed include hydrolysis of NO_2 on various surfaces,[5,13,23−35] reaction of NO_2 on soot,[36−39] reaction of HO_2 with NO_2,[40] peroxyacetyl nitrate decomposition, NO_2 abstraction of allylic hydrogen atoms, and direct emission from combustion processes.[17,41−43] Despite the large amount of research which has been devoted to HONO, these sources remain poorly understood and difficult to study experimentally due, in part, to problems with quantifying HONO.

Several approaches have been applied to measuring gaseous HONO in laboratory systems and in the atmosphere. Differential optical absorption spectroscopy (DOAS) is a sensitive and specific method which requires a HONO reference spectrum[44] generated using a high-purity source of HONO. Although various methods of gaseous HONO synthesis have been reported,[45−47] generation of HONO containing low levels of impurities, particularly NO_2, is difficult. Another group of methods for HONO quantification involves the use of denuders and NO_x detectors.[48,29] Denuder methods rely on the efficiency and specificity of each denuder and have additional uncertainties associated with obtaining HONO from the difference between two numbers which are often very similar in magnitude.Wet chemical techniques such as ion chromatography or reduction of dissolved nitrite to NO have also been used.[22,46,49] Finally, atmospheric pressure ionization mass spectrometry has been used to measure HONO[15] via MS-MS of the Cl^-·HONO adduct formed when CCl_4 is added to the discharge region in which the ions are generated.

We report here a unique procedure for quantification of HONO in laboratory systems which utilizes the reaction of gaseous HONO with excess HCl to produce ClNO:

$$\mathrm{HONO + HCl \rightarrow ClNO + H_2O} \qquad (1)$$

The product nitrosyl chloride can be synthesized in high purity for calibrations and is easily measured using FTIR.

The reaction of HONO with HCl on sulfuric acid surfaces[50−52] or on ice[53] has been reported, and on ice the yield of ClNO is 100% with respect to the HONO reacted.[53] We show that this stoichiometry also applies to the reaction 1 and report an upper limit for the rate constant of reaction 1 in the gas phase at room temperature.

* To whom correspondence should be addressed: e-mail BJFINLAY@UCI.EDU; phone (949) 824-7670; fax (949) 824-3168.

† Institut für Atmosphärische Chemie, Jülich, Germany.

10.1021/jp992890e CCC: $19.00
Published on Web 12/17/1999

II. Experimental Section

Apparatus. The apparatus used to perform the HONO titration experiments has been described in detail by De Haan et al.[54] Briefly, it is a 561 L stainless steel and aluminum chamber with two sets of White optics[55] for long path UV/visible and FTIR spectroscopy, (Mattson, Infinity AR). The base path length of the White cell is 2 m, with all experiments performed at a total path length of 52.53 ± 0.07 m in both UV/visible and IR spectroscopy. UV/visible spectroscopy was carried out using a high-pressure Xenon arc lamp (Oriel, 75 W, O_3-free, model 6263) and a grating spectrograph (Jobin-Yvon, Spex, model HR460) equipped with a diode array detector (Princeton Instruments, Inc., model RY-1024). The chamber has a surface area-to-volume ratio of $S/V = 8\ m^{-1}$ and is evacuable to $\sim 1 \times 10^{-3}$ Torr. It is equipped with a relative humidity gauge (Vaisala, type HMP432), and the internal walls are coated with an inert halocarbon wax (Halocarbon Products Corp., Series 1500) to minimize loss of reactants at the walls.

Generation of HONO and Reference Gases. Gaseous nitrous acid was generated by flowing N_2 (Oxygen Service Company, ultrahigh purity, 99.999%) over the surface of an aqueous solution of 5.2 M HCl (prepared from Fisher HCl, 37.5%, 12.1 M) held at 0 °C with an ice bath. HCl (g) and water vapor in N_2 flowed upward through a glass cell with a 9 cm diameter porous glass frit holding a bed of ~20 g $NaNO_2$ powder (Fisher, 99.6%) moistened with Nanopure water (18.2 MΩ·cm). The optimum flow rate was $\cong 2.8\ L\ min^{-1}$, with lower flow rates yielding more NO_2 impurity in the output. In some of the experiments, gaseous HONO was synthesized using "super free-flowing" $NaNO_2$ (Aldrich, 99.5%). In these cases, no water was added to the surface of the powder and lower flow rates were used, resulting in less NO_2 and water vapor, but some unreacted HCl, in the output. HONO flowed directly from the generation apparatus into the chamber through a port in a side panel.

Nitrosyl chloride was synthesized using a mixture of ~100 Torr Cl_2 (Matheson, 99.5%) and a slight excess (>200 Torr) of NO (Matheson, 99%). The mixture was first condensed at 77 K in the coldfinger of a 5 L bulb, then allowed to warm to room temperature. Reaction to form ClNO occurs primarily in the liquid phase as the mixture warms. After several such reaction cycles, the gaseous ClNO was condensed at 195 K with a dry ice−acetone bath and the excess NO was pumped away. The purity was tested using FTIR with a 32.0 or 52.5 m path length. No evidence of NO was found in the spectrum. NO_2 was sometimes observed at very low levels, <2%. The ClNO calibration was performed by adding a measured pressure of ClNO to the chamber and adding N_2 to a total pressure of ~1 atm. Successive dilutions were made by pumping the chamber down to a known total pressure and rediluting with N_2 to 1 atm.

NO_2 was synthesized by combining an excess of O_2 (Oxygen Service Co., 99.993%) with NO which had been first passed through a trap at 195 K to remove impurities such as HNO_3. The NO_2 was purified by condensing the mixture at 195 K using a dry ice−acetone bath and pumping away the excess O_2.

Gaseous HCl (Scott Specialty Gases, 99.995%) was used as a reactant in the titration. Reference spectra of HNO_3 were obtained using dry HNO_3 prepared using the vapor over a 2:1 mixture of liquid H_2SO_4:HNO_3 (H_2SO_4, Fisher, 95.7%, 18 M; HNO_3, Fisher, 70%, 15.8 M).

HONO Titration. A total of six titration experiments were performed. Continuous, simultaneous HONO measurements were made using UV/visible spectroscopy (0.27 nm resolution) and IR spectroscopy (0.5 cm^{-1} resolution). The HONO generation apparatus described above was used to flow a HONO/N_2 mixture into the evacuated chamber to an initial pressure varying from ~65 Torr to ~550 Torr and N_2 was added to a total pressure of 700 Torr. Wall loss of HONO was then monitored for 15 to 30 min by FTIR and DOAS. The titration experiment was initiated by flushing an excess of HCl (g) from a passivated glass cell of known volume into the chamber through a side panel using N_2 to a total pressure of 750 Torr. The amount of excess HCl used was at least 10 times the initial HONO concentration, which was determined in real time by DOAS using the HONO cross sections of Bongartz et al.[56,57] The loss of HONO due to reaction with HCl was followed with time by DOAS and FTIR, and ClNO formation was followed by FTIR. The loss of ClNO in the chamber under the experimental conditions was measured by following it with time after most of the HONO had reacted so that there was no formation of ClNO at these longer times. The ClNO and NO_2 concentrations were determined by calibration with pure samples of these compounds.

Another potential source of ClNO in these experiments is the reaction of HCl with NO_2, present as an impurity in the synthesis of HONO. To investigate the products of this reaction, several experiments were carried out in which known concentrations of NO_2 and HCl were flushed into the chamber, followed by filling to 1 atm with humid N_2 to replicate conditions of a typical titration experiment. NO_2 was followed by DOAS and by FTIR and ClNO and HNO_3 were followed by FTIR.

UV/Visible and IR Analyses. The DOAS approach is based on using differential cross sections rather than absolute cross sections. In the case of absolute cross sections, the Beer−Lambert law applied to complex mixtures of absorbing gases is given by eq I

$$I(\lambda) = I_o(\lambda) \times \exp[-L(\sum \sigma_i N_i + \sigma_{\text{unk}} N_i)] \qquad \text{(I)}$$

where $I(\lambda)$ is the light intensity at λ after passing through the sample, $I_o(\lambda)$ is the lamp intensity after travelling the total path length (L) with no absorbers, σ_i is the absolute absorption cross section for each species, i, N_i is the concentration of each species, and σ_{unk} represents Rayleigh scattering and broad absorptions from unknown species. UV/visible spectra can be further described as the combination of a broad, continuous absorption feature and highly wavelength-dependent, structured absorption bands. Thus, eq I can be further separated giving eq II[58]

$$I(\lambda) = I_o(\lambda) \times \exp(-L\sum \sigma'_i N_i) \times \exp(-L[\sum (\sigma_i^B N_i + \sigma_{\text{unk}} N_i)) \qquad \text{(II)}$$

where $\sigma_i = \sigma'_i + \sigma_i^B$, in which σ'_i represents the cross sections for the structured portion of species i, i.e., the differential cross section, and σ_i^B represents the cross sections for the broad portion of species i. The structured spectral features provide the specificity needed to identify and quantify each compound, and hence only the differential cross sections are used in the DOAS approach.

Taking the natural logarithm of both sides, eq II becomes

$$\ln\left(\frac{I_o}{I}\right) = L\sum \sigma'_i N_i + L\sum (\sigma_i^B N_i + \sigma_{\text{unk}} N_i) \qquad \text{(III)}$$

which is of the form

$$F(\lambda) = \sum_i (a_i \times S_i(\lambda)) + P(\lambda) \qquad \text{(IV)}$$

where $S_i(\lambda)$ are reference absorption spectra of known concentration, a_i are scaling factors for the reference spectra, and $P(\lambda)$ is a polynomial to fit the broad features. Because the recorded spectra consist of the sum of the broad features and the structured features of the absorber(s), the spectra in the form of eq IV must be fitted mathematically to determine the contributions of each species to the total spectrum. This was accomplished by minimizing the residuals between each experimental spectrum and a linear combination of the reference spectra of all the contributing species to obtain a model spectrum, $F(\lambda)$, based on eq IV.[59] HONO and NO_2 concentrations were determined by fitting UV/visible spectra with HONO and NO_2 reference spectra and a third-order polynomial in the 340−380 nm region. The published cross sections of Bongartz et al.[56,57] were used for HONO after first converting to 0.27 nm resolution by convolution with the instrument function of the grating spectrograph.

Equation IV can be applied to IR spectroscopy as well because rovibrational spectra are structured, while the baseline is treated as a broad feature. Hence, IR spectra were analyzed using eq IV with polynomials of zero to second order to simulate the baseline and with reference spectra for HONO, HNO_3, and H_2O. The use of an aqueous solution of HCl for the synthesis of HONO produced a significant amount of water vapor in the chamber so that the relative humidity during the experiments varied from ∼10% to 30%. This water vapor caused interferences in the IR spectra in both HONO and ClNO regions. The interfering rotational structure from water vapor was accounted for by fitting the experimental spectra to a reference water spectrum taken at a similar water vapor concentration.

III. Results and Discussion

Typical IR spectra showing the loss of HONO and production of ClNO are shown in Figure 1. The HONO band centered at 1263 cm^{-1} (ν_3, *trans*-HONO) is shown in Figure 1a at $t = 0$, as well as at 1 h and 3 h after HCl addition. Figure 1b shows the corresponding production of ClNO (ν_1, centered at 1799 cm^{-1}) at the same times. UV/visible spectra showing HONO loss at approximately the same times are shown in Figure 2. The fitting procedure described above was applied to the spectra in Figures 1 and 2, followed by subtraction of the interfering compounds leaving the HONO and ClNO spectra shown.

Stoichiometry of Reaction 1. For each experiment, the change in the concentrations of ClNO (determined by FTIR) and HONO (determined by DOAS) were calculated relative to the time when HCl was added. The increase in [ClNO] was plotted against the decrease in [HONO] for equal time intervals and the slope obtained for each experiment. Using a numerical integration program, ACUCHEM,[60] the HONO and ClNO time traces were modeled with wall losses set to experimentally observed values as well as with wall losses set to zero. Comparison of the two model runs showed that wall loss effects were negligible until ∼54 min; thus, all stoichiometry plots were obtained using data from ≤54 min. A slope of unity indicates that one ClNO forms for every HONO destroyed, i.e., a one-to-one stoichiometry for reaction 1. The slopes obtained for these stoichiometry plots are shown in Table 1 (column 4) for all experiments, with the average equal to 0.9 ± 0.2 (1σ). Although there is low precision between experiments, on average one ClNO molecule forms for every HONO molecule reacted. This is consistent with the results of Fenter and Rossi,[53] who observed

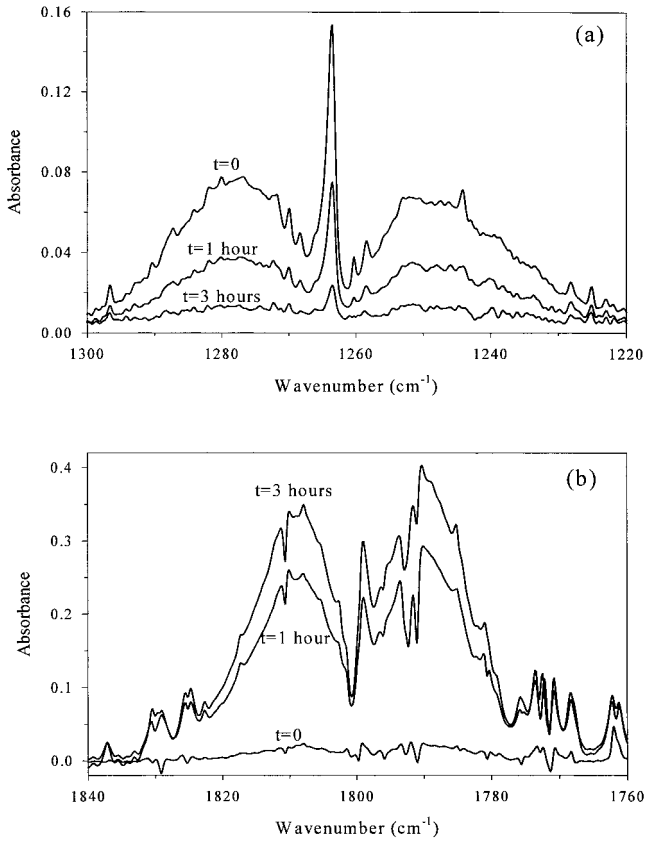

Figure 1. Infrared spectra showing (a) the loss of HONO (1263 cm^{-1}) and (b) the increase in ClNO (1799 cm^{-1}) with time upon addition of excess HCl (7.93×10^{14} molecules cm^{-3}) during a typical experiment (#2). The absorption cross section for ClNO at 1799 cm^{-1} with 0.5 cm^{-1} resolution determined in these studies using authentic ClNO was $(1.08 \pm 0.11) \times 10^{-18}$ cm^2 $molecule^{-1}$, base 10 (2σ).

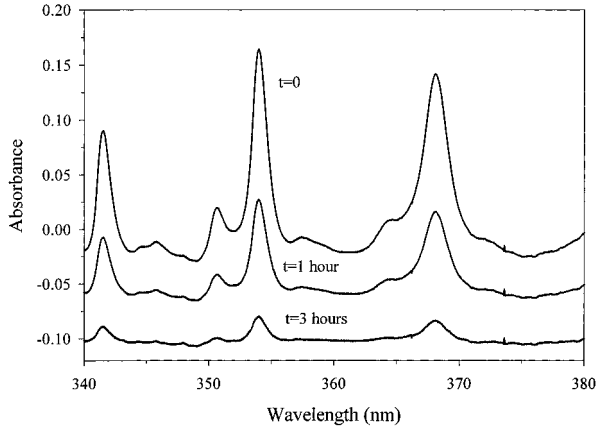

Figure 2. UV/visible spectra of gaseous HONO corresponding to approximately the same times as the IR spectra shown in Figure 1. At $t = 0$ $[HONO]_o = 7.6 \times 10^{13}$ molecules cm^{-3}, at $t = 1$ h [HONO] = 3.6×10^{13} molecules cm^{-3}, and at $t = 3$ h [HONO] = 9.3×10^{12} molecules cm^{-3}. Spectra are offset on *y*-axis for clarity.

a one-to-one stoichiometry for reaction of HONO with HCl on an ice substrate.

Other possible sources of ClNO in this system were considered. The reaction of NO_2 impurity, present in the HONO, with HCl was examined

$$2NO_2 + HCl \rightarrow ClNO + HNO_3$$

To test this possibility, concentrations of HCl, NO_2, and H_2O typical of those in the titration experiments were introduced

TABLE 1: Summary of Kinetic and Concentration Data for HONO Titration Experiments

1 exp. no.	2 $[HCl]_o$ (molecules cm^{-3})	3 initial HONO (molecules cm^{-3}) from DOAS analysis[a]	4 stoichiometry plot slope $(-\Delta[ClNO]/\Delta[HONO])$	5 k_1 from FTIR analysis of HONO[b] (cm^3 molecule^{-1} s^{-1})	6 k_1 from DOAS analysis of HONO (cm^3 molecule^{-1} s^{-1})	7 $[HONO]_o$ (molecules cm^{-3}) determined by titration	8 percent deviation (col3−col7)/col3 × 100%
1	9.35×10^{14}	1.05×10^{14}	1.3	3.05×10^{-19}	2.91×10^{-19}	9.35×10^{13}	11%
2	7.93×10^{14}	7.55×10^{13}	0.76	2.01×10^{-19}	2.21×10^{-19}	7.15×10^{13}	5%
3	8.48×10^{14}	6.84×10^{13}	0.77	1.83×10^{-19}	2.16×10^{-19}	6.61×10^{13}	3%
4	8.41×10^{14}	3.59×10^{13}	1.0	1.21×10^{-19}	1.23×10^{-19}	4.52×10^{13}	−26%[d]
5	8.53×10^{14}	3.28×10^{13}	0.74	1.19×10^{-19}	1.07×10^{-19}	4.07×10^{13}[c]	−24%[d]
6	8.41×10^{14}	2.10×10^{13}	0.66	1.90×10^{-19}	1.61×10^{-19}	1.61×10^{13}	23%[d]
avg ± std dev			0.9 ± 0.2 (1σ)	$(1.86 \pm 1.36) \times 10^{-19}$ (2σ)	$(1.87 \pm 1.39) \times 10^{-19}$ (2σ)		−1% ± 39% (2σ)

[a] These values of $[HONO]_o$ were determined using the revised UV/visible cross sections of Bongartz et al.[56,57] at the point just before addition of excess HCl. [b] Each rate constant in column 5 is an average of the rate constants obtained from the natural log plots using the three HONO infrared absorption peaks centered at 790, 852, and 1263 cm^{-1}. [c] Experiment 5 had insufficient data at long times to measure the wall loss of ClNO. Thus, the average k_2 from the other experiments was used, $k_2^{avg} = 1.69 \times 10^{-5}$ s^{-1}. [d] HCl from the HONO generation apparatus was present at the beginning of these experiments which may have affected the rate of HONO loss before excess HCl addition.

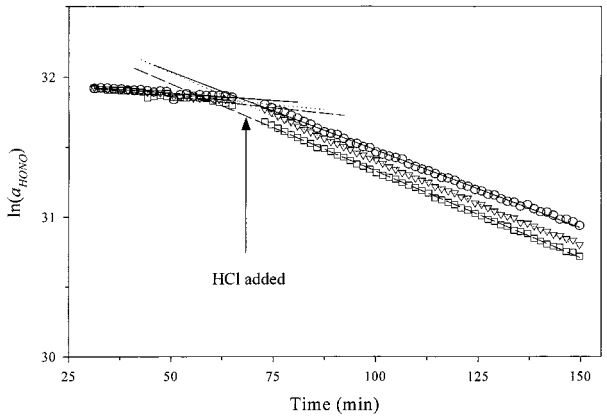

Figure 3. Typical plots of $\ln(a_{HONO})$ using the IR data versus time (experiment 3). Circles (○) are for the 790 cm^{-1} peak, inverted triangles (▽) are for the 852 cm^{-1} peak, and squares (□) are for the 1263 cm^{-1} peak. The symbols do not lie on top of each other because different reference HONO spectra were used for each infrared peak.

into the chamber and the formation of ClNO followed with time. Under conditions similar to those of experiments 1−6, only small yields of ClNO, <2% relative to the ClNO formed during a titration experiment with similar concentrations of NO_2, were produced. Thus, reaction of NO_2 with HCl cannot be a significant source of ClNO in these HONO + HCl experiments. While some contribution from other unrecognized secondary reactions cannot be ruled out with certainty, no additional products were observed in the infrared spectrum.

Kinetics of Reaction 1. The time dependence of HONO and ClNO during the reaction of HONO with HCl can be used to measure the rate constant for reaction 1. Reactions 1−3 describe this system:

$$HONO + HCl \xrightarrow{k_1} ClNO + H_2O \quad (1)$$

$$ClNO \xrightarrow{k_2} \text{products} \quad (2)$$

$$HONO \xrightarrow{k_3} \text{products} \quad (3)$$

The time dependence of HONO is described by its loss by reaction with HCl, reaction 1, as well as its loss to the walls, reaction 3. Although there may be a small contribution from photodissociation of HONO and ClNO by the Xe arc lamp used for DOAS, these are small compared to the total loss; for example, the net rate of loss of ClNO at ∼10% RH is not significantly different with or without the DOAS beam. HCl was used in excess so that its concentration remained approximately constant (≤6% loss over the times studied here). Thus, the integrated rate equation for HONO is given by eq V

$$[HONO] = [HONO]_o e^{-(k_1[HCl]_o + k_3)t} \quad (V)$$

where k_1 is the second-order rate constant for the reaction of HONO with HCl, k_3 is the first-order rate constant for HONO loss in the chamber, $[HCl]_o$ is the initial HCl concentration, and $[HONO]_o$ is the initial HONO concentration before addition of excess HCl. To obtain k_1 from eq V, $\ln(a_{HONO})$, where a_{HONO} are the scaling factors in eq IV, was plotted versus time, the slope of which is equal to $-(k_1[HCl]_o + k_3)$. The first-order loss of HONO, k_3, was obtained experimentally by following HONO by FTIR and DOAS before HCl was added for each experiment. $[HCl]_o$ is known for each experiment, thus k_1 can be determined for each experiment from the slope after addition of HCl.

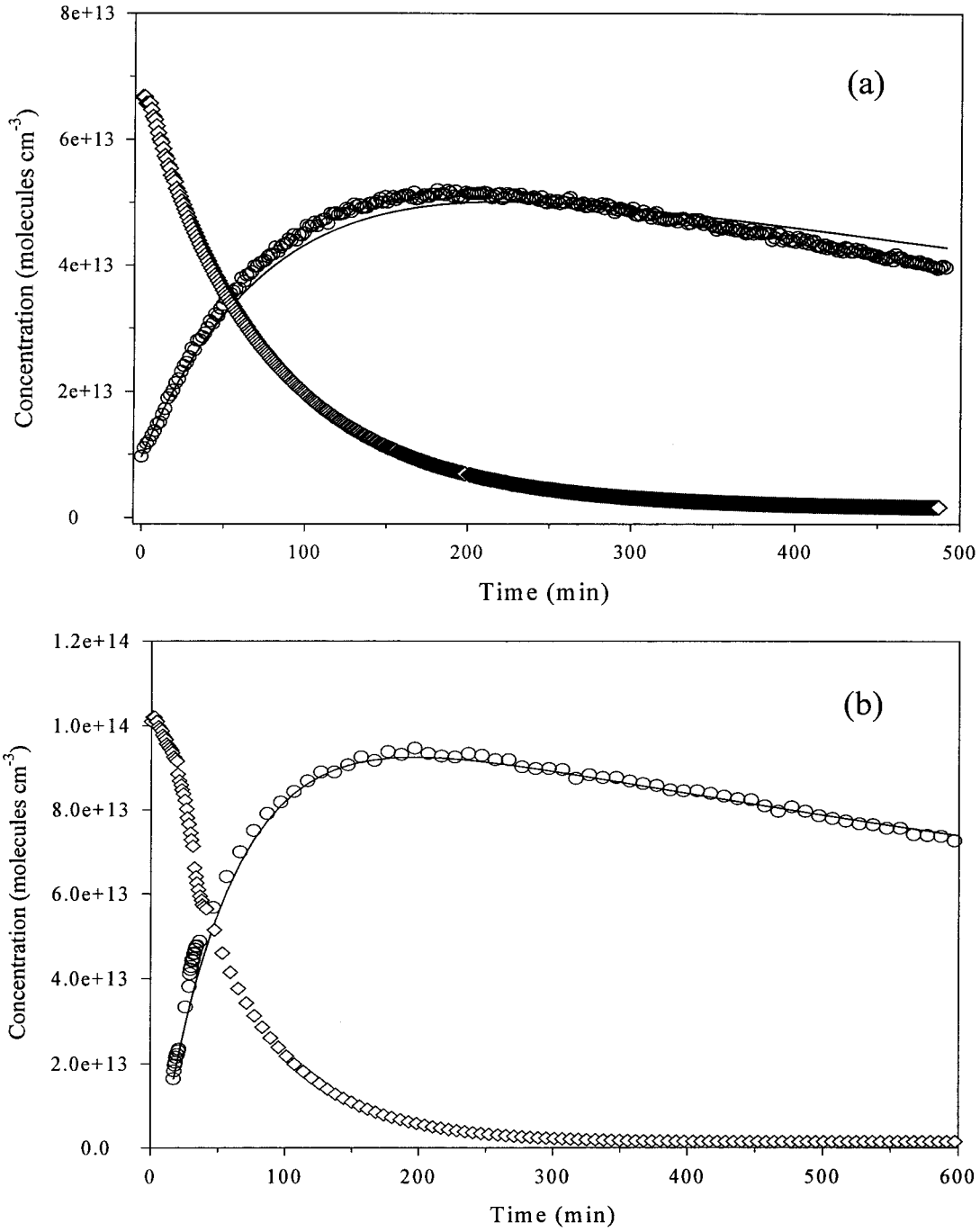

Figure 4. Time profiles for HONO measured by DOAS (diamonds (◊)) and ClNO by FTIR (circles (○)) during typical experiments: (a) experiment 3, (b) experiment 1. Errors (2σ) for ClNO and HONO were derived from the error in the peak fitting procedure and are equal to or less than the size of the data points. Regression of the ClNO data is shown as solid lines.

Figure 3 shows typical plots of $\ln(a_{HONO})$ versus time using the IR peaks at 790, 852, and 1263 cm^{-1}. Table 1 summarizes the values obtained for k_1 by FTIR (column 5) using this approach. Column 6 of Table 1 gives the values of k_1 obtained using the same analysis but using the DOAS HONO data. The average values for k_1 using the two measurement methods for HONO, $k_1 = (1.9 \pm 1.4) \times 10^{-19}$ cm^3 molecule^{-1} s^{-1} (2σ) by FTIR and $k_1 = (1.9 \pm 1.4) \times 10^{-19}$ cm^3 molecule^{-1} s^{-1} (2σ) using DOAS, are in excellent agreement, although the error bars for each are large. The overall rate constant using both analytical techniques for HONO analysis is $k_1 = (1.9 \pm 1.3) \times 10^{-19}$ cm^3 molecule^{-1} s^{-1} (2σ). Values of k_3 ranged from (1.8−6.5) $\times 10^{-5}$ s^{-1} in these experiments; this represented from 6 to 39% of the total HONO loss in individual experiments. As expected, the largest percentages were in the runs in which there was unreacted HCl present initially in the HONO.

Karlsson and Ljungström[61] studied the reverse reaction, ClNO hydrolysis, and reported an upper limit for the rate constant for reaction −1

$$\mathrm{ClNO} + \mathrm{H_2O} \xrightarrow{k_{-1}} \mathrm{HONO} + \mathrm{HCl} \qquad (-1)$$

to be $k_{-1}(296\ \mathrm{K}) \leq (7.4 \pm 2.4) \times 10^{-22}$ cm^3 molecule^{-1} s^{-1}. Using the calculated value of the equilibrium constant of $K_1(296\ \mathrm{K}) = 1.25 \times 10^4$ based on the published Gibbs free energy for the more stable *trans*-HONO,[62] the upper limit for the rate constant of the forward reaction 1 is thus $k_1(296\ \mathrm{K}) \leq 9.3 \times$

10^{-18} cm^3 molecule^{-1} s^{-1}. Our measured value of $k_1 = (1.9 \pm 1.3) \times 10^{-19}$ cm^3 molecule^{-1} s^{-1} (2σ) for a temperature of 297 $\pm$ 1 K is consistent with this reported upper limit. As discussed below, a heterogeneous contribution to reaction 1 cannot be ruled out, and hence this value should be taken as an upper limit to the gas phase rate constant.

HONO Quantification. The time dependence of the concentration of ClNO is determined by its production in reaction 1 and the wall loss in reaction 2. The integrated rate equation for ClNO, with [HCl] constant, is given by eq VI

$$[\mathrm{ClNO}] = \frac{k_1[\mathrm{HONO}]_o[\mathrm{HCl}]_o}{k_2 - k_1[\mathrm{HCl}]_o - k_3}(e^{-(k_1[\mathrm{HCl}]_o + k_3)t} - e^{-k_2 t}) + [\mathrm{ClNO}]_o \quad \text{(VI)}$$

In eq VI, k_2 is the rate constant for first-order ClNO loss and $[\mathrm{ClNO}]_o$ is the initial ClNO concentration. The slow hydrolysis of ClNO, reaction -1, was treated as first-order ClNO loss included in the parameter k_2 due to the high concentrations of water used. While $[\mathrm{ClNO}]_o$ should theoretically be zero, in some cases some unreacted HCl passed through the HONO generation apparatus, causing small amounts of ClNO to form before the addition of excess HCl. The value of $[\mathrm{HONO}]_o$ is treated as unknown and is obtained by regression analysis of ClNO data.

The experimental ClNO data were fitted to eq VI using regression analysis in which the value of $[\mathrm{HONO}]_o$ was optimized, while $[\mathrm{HCl}]_o$, k_1, k_2, and k_3 were fixed at the values measured in that experiment. The value of k_2 in eq VI was determined by plotting ln[ClNO] versus time for later times in the experiment when $\geq$95% of the initial HONO had reacted. Under these conditions, new formation of ClNO was minimal and ClNO loss was dominant. Values of k_2 ranged from $(0.7-2) \times 10^{-5}$ s^{-1} in these experiments, which corresponded to 4$-$11% of the total measured loss rates for HONO. The effect of changes in HCl concentration during an experiment was examined by modeling the system with and without HCl wall loss.[60] The small change in HCl concentration over the time of an experiment ($\leq$6%) did not significantly affect the value of $[\mathrm{HONO}]_o$ determined by regression (<2%).

Figure 4 shows typical experimental data for the decrease in HONO (determined by DOAS) and production of ClNO (determined by IR) with time. Also shown is the regression of the ClNO data using eq VI with $[\mathrm{HONO}]_o$ treated as an adjustable parameter whose value is determined by optimizing the fit to the data. In these experiments, the fitting procedure gave $[\mathrm{HONO}]_o = 6.6 \times 10^{13}$ molecules cm^{-3} (Figure 4a) and $[\mathrm{HONO}]_o = 9.4 \times 10^{13}$ molecules cm^{-3} (Figure 4b), in good agreement with the values of 6.8×10^{13} and 1.1×10^{14} molecules cm^{-3}, respectively, determined by DOAS.

Table 1 summarizes the initial HONO concentrations obtained by the titration method (column 7) as well as those determined by DOAS (column 3) using the cross sections of Bongartz et al.[56,57] The values determined by the titration method deviate from those determined by DOAS in individual experiments by -26 to $+23$% (column 8). The largest deviations occur for those experiments in which unreacted HCl was present initially from the HONO generation; in these experiments the initial HONO concentrations were also smaller so that the absolute increase in ClNO on adding excess HCl was also smaller. In addition, the differences in the first-order rates of HONO loss before and after adding excess HCl were smaller. However, the average deviation over all experiments is only 1%, but with a large uncertainty (39%, 2σ). The experiments with the highest deviations, experiments 4$-$6, were those in which dry, "free-flowing" $NaNO_2$ was used in the HONO generation, resulting in some unreacted HCl passing through the generator and into the chamber before the titration began. The regression fits in these experiments also showed the largest deviation from the ClNO data. The average of the percent deviations, however, is close to zero, indicating that the $[\mathrm{HONO}]_o$ values determined by the titration deviate both positively and negatively, i.e., there is no apparent systematic error.

The gas-phase reaction of HONO with HCl to produce ClNO has not been reported in the literature to our knowledge. However, the heterogeneous reaction of HONO with HCl on ice and concentrated sulfuric acid solution substrates has been studied by several groups with a one-to-one stoichiometry as found in the present studies.[50−53] While the spectroscopic techniques used here detect only gaseous species, we investigated a possible contribution from a wall reaction by carrying out three titration experiments in a 7.6 L, glass long path cell (S/V = 40 m^{-1}). The rate constant obtained for reaction 1 in this cell was found to be $k_1^{(7.6\mathrm{L\ cell})} \cong (3 \pm 2) \times 10^{-19}$ cm^3 molecule^{-1} s^{-1} (2σ), within experimental error of that obtained in the much larger chamber, suggesting that a surface reaction does not predominate in these experiments. However, given the relatively large errors in our values of k_1 and that similar reactions of HCl, e.g., with $ClONO_2$ and N_2O_5, occur at least in part on surfaces,[63] a heterogeneous component cannot be ruled out.

IV. Summary

The gas-phase reaction of HONO with HCl has been shown to form ClNO with a stoichiometry of 0.9 ± 0.2 (1σ), i.e., within experimental error of unity. Although the reaction is slow, $k_1 \leq (1.9 \pm 1.3) \times 10^{-19}$ cm^3 molecule^{-1} s^{-1} (2σ) at 297 K, it has been shown to be a useful method for quantifying HONO in laboratory systems, since calibration for ClNO can be readily carried out. While the direct use of the available IR cross sections for HONO in the literature is a possible alternative, there are significant discrepancies in the reported IR cross sections.[64] This method has the advantage over UV/visible spectroscopy that it does not require the more complex data analysis associated with DOAS and allows the simultaneous determination of the other species, such as HNO_3, which cannot be measured by DOAS. It is also a more direct and specific method than the denuder and NO_x detector approaches.

Acknowledgment. The authors thank Jorg Meyer for glassblowing the experimental apparatus used for HONO generation and Jochen Stutz, M. T. Leu, and P. Shepson for helpful discussions. We also thank the California Air Resources Board (Contract No. 97-311) and National Science Foundation (Award No. ATM-9496240) for support of this research.

References and Notes

(1) Chan, W. H.; Nordstrom, R. J.; Calvert, J. G.; Shaw, J. H. *Chem. Phys. Lett.* **1976**, *37*, 441.

(2) Winer, A. M.; Biermann, H. W. *Res. Chem. Intermed.* **1994**, *20*, 423.

(3) Harrison, R. M.; Peak, J. D.; Collins, G. M. *J. Geophys. Res.* **1996**, *101*, 14429.

(4) Wiesen, P.; Kleffmann, J.; Kurtenbach, R.; Becker, K. H. *Faraday Discuss.* **1995**, *100*, 121.

(5) Kleffmann, J.; Becker, K. H.; Wiesen, P. *Atmos. Environ.* **1998**, *32*, 2721.

(6) Kleffmann, J.; Becker, K. H.; Wiesen, P. *J. Chem. Soc., Faraday Trans.* **1998**, *94*, 3289.

(7) Crutzen, P. J. *Q. J. R. Meterol. Soc.* **1970**, *96*, 320.

(8) Prather, M.; Derwent, R.; Ehhalt, D.; Fraser, P.; Sanhueza, E.; Zhou, X. Climate Change 1995 in *The Science of Climate Change, Contribution*

of Working Group I to the Second Assessment Report of the Intergovernmental Panel on Climate Change; Houghton, J. T., Meira Filho, L. G., Callander, B. A., Harris, N., Kattenberg, A., Maskell, K., Eds.; Cambridge University Press: New York, 1996; chapter 2.

(9) Khalil, M. A. K.; Rasmussen, R. A. *J. Geophys. Res.* **1992**, *97*, 14651.

(10) Bouwman, A. F.; Van der Hoek, K. W.; Olivier, J. G. J. *J. Geophys. Res.* **1995**, *100*, 2785.

(11) Rasmussen, T. R.; Brauer, M.; Kjærgaard, S. *Am. J. Respir. Crit. Care Med.* **1995**, *151*, 1504.

(12) Beckett, W. S.; Russi, M. B.; Haber, A. D.; Rivkin, R. M.; Sullivan, J. R.; Tameroglu, Z.; Mohsenin, V.; Leaderer, B. P. *Environ. Health Perspect.* **1995**, *103*, 372.

(13) Pitts, J. N., Jr.; Wallington, T. J.; Biermann, H. W.; Winer, A. W. *Atmos. Environ.* **1985**, *19*, 763.

(14) Brauer, M.; Ryan, P. B.; Suh, H. H.; Koutrakis, P.; Spengler, J. D.; Leslie, N. P.; Billick, I. H. *Environ. Sci. Technol.* **1990**, *24*, 1521.

(15) Spicer, C. W.; Kenny, D. V.; Ward, G. F.; Billick, I. H. *J. Air Waste Manage. Assoc.* **1993**, *43*, 1479.

(16) Spengler, J. D.; Brauer, M.; Samet, J. M.; Lambert, W. E. *Environ. Sci. Technol.* **1993**, *27*, 841.

(17) Vecera, Z.; Dasgupta, P. K. *Intern. J. Environ. Anal. Chem.* **1994**, *56*, 311.

(18) Pitts, J. N., Jr.; Grosjean, D.; Van Cauwenberghe, K.; Schmid, J. P.; Fitz, D. R. *Environ. Sci. Technol.* **1978**, *12*, 946.

(19) Perner, D.; Platt, U. *Geophys. Res. Lett.* **1979**, *6*, 917.

(20) Lammel, G.; Cape, J. N. *Chem. Soc. Rev.* **1996**, *25*, 361.

(21) Febo, A.; Perrino, C.; Allegrini, I. *Atmos. Environ.* **1996**, *30*, 3599.

(22) Vecera, Z.; Dasgupta, P. K. *Environ. Sci. Technol.* **1991**, *25*, 255.

(23) Sakamaki, F.; Hatakeyama, S.; Akimoto, H. *Int. J. Chem. Kinet.* **1983**, *15*, 1013.

(24) Pitts, J. N., Jr.; Sanhueza, E.; Atkinson, R.; Carter, W. P. L.; Winer, A. M.; Harris, G. W.; Plum, C. N. *Int. J. Chem. Kinet.* **1984**, *16*, 919.

(25) Akimoto, H.; Takagi, H.; Sakamaki, F. *Int. J. Chem. Kinet.* **1987**, *19*, 539.

(26) Svensson, R.; Ljungström, E.; Lindqvist, O. *Atmos. Environ.* **1987**, *21*, 1529.

(27) Jenkin, M. E.; Cox, R. A.; Williams, D. J. *Atmos. Environ.* **1988**, *22*, 487.

(28) Lammel, G.; Perner, D. *J. Aerosol Sci.* **1988**, *19*, 1199.

(29) Febo, A.; Perrino, C. *Atmos. Environ.* **1991**, *25A*, 1055.

(30) Notholt, J.; Hjorth, J.; Raes, F. *Atmos. Environ.* **1992**, *26A*, 211.

(31) Junkermann, W.; Ibusuki, T. *Atmos. Environ.* **1992**, *26A*, 3099.

(32) Bambauer, A.; Brantner, B.; Paige, M.; Novakov, T. *Atmos. Environ.* **1994**, *28*, 3225.

(33) Mertes, S.; Wahner, A. *J. Phys. Chem.* **1995**, *99*, 14000.

(34) Goodman, A. L.; Underwood, G. M.; Grassian, V. H. *J. Phys. Chem. A* **1999**, *103*, 7217.

(35) Barney, W. S.; Finlayson-Pitts, B. J. *J. Phys. Chem. A*, in press.

(36) Ammann, M.; Kalberer, M.; Jost, D. T.; Tobler, L.; Rössler, E.; Piguet, D.; Gäggeler, H. W.; Baltensperger, U. *Nature* **1998**, *395*, 157.

(37) Gerecke, A.; Thielmann, A.; Gutzwiller, L.; Rossi, M. J. *Geophys. Res. Lett.* **1998**, *25*, 2453.

(38) Longfellow, C. A.; Ravishankara, A. R.; Hanson, D. R. *J. Geophys. Res.* **1999**, *104*, 13833.

(39) Kalberer, M.; Ammann, M.; Arens, F.; Gäggeler, H. W.; Baltensperger, *J. Geophys. Res.* **1999**, *104*, 13825.

(40) Tyndall, G. S.; Orlando, J. J.; Calvert, J. G. *Environ. Sci. Technol.* **1995**, *29*, 202.

(41) Pitts, J. N., Jr.; Biermann, H. W.; Winer, A. M.; Tuazon, E. C. *Atmos. Environ.* **1984**, *18*, 847.

(42) Kirchstetter, T. W.; Harley, R. A.; Littlejohn, D. *Environ. Sci. Technol.* **1996**, *30*, 2843.

(43) Finlayson-Pitts, B. J.; Pitts, J. N., Jr. *Chemistry of the Upper and Lower Atmosphere*, Academic Press: San Diego, 2000.

(44) Stutz, J.; Kim, E. S.; Platt, U.; Bruno, P.; Perrino, C.; Febo, A. *J. Geophys. Res.*, submitted.

(45) Febo, A.; Perrino, C.; Gherardi, M.; Sparapani, R. *Environ. Sci. Technol.* **1995**, *29*, 2390.

(46) Taira, M.; Kanda, Y. *Anal. Chem.* **1990**, *62*, 630.

(47) Braman, R. S.; de la Cantera, M. A. *Anal. Chem.* **1986**, *58*, 1533.

(48) Ferm, M.; Sjödin, Å. *Atmos. Environ.* **1985**, *19*, 979.

(49) Harrison, R. M.; Peak, J. D.; Collins, G. M. *J. Geophys. Res.* **1996**, *101*, 14429.

(50) Zhang, R.; Leu, M.-T.; Keyser, L. F. *J. Phys. Chem.* **1996**, *100*, 339.

(51) Burley, J. D.; Johnston, H. S. *Geophys. Res. Lett.* **1992**, *19*, 1363.

(52) Longfellow, C. A.; Imamura, T.; Ravishankara, A. R.; Hanson, D. R. *J. Phys. Chem. A* **1998**, *102*, 3323.

(53) Fenter, F. F.; Rossi, M. J. *J. Phys. Chem.* **1996**, *100*, 13765.

(54) De Haan, D. O.; Brauers, T.; Oum, K. W.; Stutz, J.; Nordmeyer, T.; Finlayson-Pitts, B. J. *Int. Rev. Phys. Chem.*, **1999**, *18*, 343.

(55) White, J. U. *J. Opt. Soc. Am.* **1942**, *32*, 285.

(56) Bongartz, A.; Kames, J.; Welter, F.; Schurath, U. *J. Phys. Chem.*, **1991**, *95*, 1076.

(57) Bongartz, A.; Kames, J.; Schurath, U.; George, Ch.; Mirabel, Ph.; Ponche, J. L. *J. Atmos. Chem.* **1994**, *18*, 149.

(58) Stutz, J.; Platt, U. *Appl. Optics* **1996**, *35*, 6041.

(59) Gomer, T.; Brauers, T.; Heintz, F.; Stutz, J.; Platt, U. MFC Version 1.98, 1995.

(60) Braun, W.; Herron, J. T.; Kahaner, D. K. *Int. J. Chem. Kinet.* **1988**, *20*, 51.

(61) Karlsson, R. S.; Ljungström, E. B. *Environ. Sci. Technol.* **1996**, *30*, 2008.

(62) Chase, M. W., Jr.; Davies, C. A.; Downey, J. R.; Jr., Frurip; D. J.; McDonald, R. A.; Syverud, A. N. *J. Phys. Chem. Ref. Data*, *14* (Suppl. 1), **1985**.

(63) Leu, M. T.; Hatakeyama, S.; Hsu, K.-J. *J. Phys. Chem.* **1989**, *93*, 5778.

(64) Barney, W. S.; Wingen, L. M.; Lakin, M. J.; Brauers, T.; Stutz, J.; Finlayson-Pitts, B. J., submitted to *J. Phys. Chem.*